doi:10.36487/ACG_repo/2063_94

Multi-attribute microseismic analysis to evaluate the evolution of in situ stress: imaging the complex relationship between stress and structure

I Nizkous ESG Solutions, Canada

L Smith-Boughner ESG Solutions, Canada

V Shumila ESG Solutions, Canada

W de Beer ESG Solutions, Australia

D Angus ESG Solutions, Canada

Abstract

Safe operations in the mining environment require mitigation of geomechanical risks through monitoring of production induced micro earthquakes. In this study we assess dynamic stress changes in an underground block caving mine in a tectonically active area during peak production activity and a following short period of relative inactivity. We analyse the collective behaviour of microseismic events (Dynamic Parameters Analysis or DPA) together with passive seismic tomography and stress inversion to get an integrated picture of the complex stress evolution processes occurring within the mine. These approaches provide complementary information for interpretation of the complex spatial and temporal stress evolution. DPA shows a cyclical process of loading and stress relaxation in the abutments of the cave during the period of study. Seismic tomography recovers compressional velocity variations correlating with the stress field behaviour observed in DPA. A region of high velocity within the rock mass is observed to undergo a loading process with local stress increase, while a region of low velocity rock mass undergoes stress relaxation with high intensity plastic deformation. Seismic moment tensor mechanisms show uniformity in the south abutment of the cave with predominantly tensile crack closure mechanism, which coincides with the region of low velocity. The high velocity region exhibits some tensile fracture opening with consistent tensile fracture closure failure type along the abutments of the cave. The principal stress directions vary around the mine abutment and display an additional level of complexity related to vertical distribution of the events. The maximum principal stress $\sigma 1$ in the south abutment of the cave appears to be consistently vertical.

1 Introduction

Monitoring of underground mining activity is a mandatory aspect of continuous safe operations. In seismically active mines, all the aspects of mining production and development are accompanied by seismic monitoring with appropriate action protocols to minimize geohazards risk, as well as damage to infrastructure and personnel injury. As mentioned previously, seismicity in mines consist of micro earthquakes induced by mining activities. The seismic activity is recorded with seismic sensors that have been permanently or temporally installed in the mine excavations.

With development of microseismic technology, determination of the location of microearthquake is only the initial step in the analysis that indicates stress concentration areas but does not provide details about spatial and temporal stress evolution. Characterization of collective behaviour of seismicity (Kostrov & Das 1988; Ben-Zion 2008) allows to quantify the similarities in the source of microseismic events in time and spatially and group these events in the way to describe rock volume behaviour. This method, referred below as Dynamic Parameters Analysis (DPA), is based on the concept of seismic stress field change that

is preserved in the recorded seismicity. The approach is successfully used to describe dynamic stress and deformation states of the rock mass in mines (Smith-Boughner et al. 2017; Veigas et al. 2018; Urbancic et al. 2015).

On the other hand, as shown by several authors (e.g., Young & Maxwell 1992; Westman et al. 2012; Ma et al. 2016; Mercier et al. 2015; Baig et al. 2017), passive seismic tomography and mapping of seismic velocity variation can be used as a proxy for rock stress behaviour, as increase in stress in a rock volume causes closure of micro fractures and reduction of the pore space, which result in increase of the stiffness on the rock mass and therefore increase of seismic velocities. Decrease of seismic velocities can be attributed to areas of stress relaxation, damaged rock and high level of plastic deformations.

In this study we combine advanced microseismic analysis methods to examine dynamic stress evolution in the cave mine located in the area of high tectonic stresses. Presence of extensive geophones network in the mine and relatively high seismic activity allow us to apply travel time tomography to track compressional seismic velocity changes and therefore related stress variation and utilize the advantages of DPA approach for rock mass state characterization, which requires statistically representative microseismic events data set. We also perform stress inversions from seismic moment tensor inversion. The stress inversions allow us to evaluate the temporal changes of the local stress directions due to the stress redistribution during mining operations.

The tree methods utilized in this paper provide insight into the problem of complexity of the stress evolution from different physical perspectives. Understanding the details of the stress field in this mining environment can be an input into stress numerical model updates and improve decision making on mine development and safety.

2 Dynamic Parameters Analysis (DPA)

Collective behaviour of microseismic events approach considers interaction between radiated seismic energy and plastic deformation related changes in the stress field that influence rupture dynamics in the rock volume. For quantitative analysis of these interaction, nearest neighbour method is used for spatial and temporal clustering of microseismic events, and for each cluster dynamic identifiers or parameters are calculated based on the total time and time span between the events, radiated energy, seismic moment and volume of rock containing microseismic events.

The dynamic parameters include Plasticity Index (PI), Stress Index (SI) and Diffusion Index (DI). These attributes describe the rock state from the perspective of deformation intensity (PI), complexity of rock failure (SI) and intensity of fracture variation with time (DI).

PI describes rock deformability. High PI values of the rock volume indicate high levels of co-seismic deformations, complex fracturing and low levels of radiated energy. Low PI corresponds to the rock volume undergoing predominantly elastic and limited deformation with time with most of the energy being radiated rather than converted into inelastic deformations.

$$PI(\Delta V, \Delta t) = \frac{\tau_T}{\tau_S} = \frac{Observation\ time}{Seismic\ relaxation\ time} \tag{1}$$

Stress field characterization is defined by SI. Rock volume containing complex network of small fractures promotes stress relaxation and dissipation, while fault activation requires increase in stress concentration before the rock failure. Thus, low SI is an indication of complex fracture network presence and localized stress dissipation mechanism. High SI associates with wide spread seismicity, stress related fracturing and fault activation with high radiated seismic energy.

$$SI(\Delta V, \Delta t) = \frac{v_S}{d_S} = \frac{Seismic\ kinematic\ viscosity}{Seismic\ diffusion} \tag{2}$$

DI describes spatial concentration of the fractures and fracture state of the rock mass and measures the spatial diffusion of seismicity that tends to follow different stress gradients. High DI relates to high rate of microseismic events occurred within a large volume of rock, while low DI represents seismic activity located within a small volume of rock and occurred during long period of time.

$$d_S = \frac{\bar{X}^2}{\dot{t}} = \frac{(Average\ consecutive\ interevent\ distance)^2}{Average\ consecutive\ intervent\ time} \quad (3)$$

3 Passive seismic tomography

Seismic tomography as an areal monitoring method, allows to reconstruct changes in seismic velocities related to the rock properties variations based on inversion of the seismic waves travel time. Variation of compressional and shear wave velocities with time describes the state of deformations and stress intensity of the rock. The technique involves iterative improvement of the starting velocity model to match observed travel times along the ray path between microseismic event source location and sensor position.

In this paper we used an improved simultaneous iterative reconstruction tomography (SIRT), originally described in Crowley et al. (2015), with error estimation and internal parameters constraint that restricts velocity variation range to predetermined acceptable values. This parameter control approach allows an assessment of the robustness and accuracy of the inversion to be determined without separate resolution test. For our dataset, the volume around cave is well-resolved and thus allows confident interpretation.

4 Stress inversion

Rock ruptures observed as microseismic events may have complex nature but can be studied and evaluated using far field seismic signals from a range of azimuths that can be inverted for simplified failure mechanism model which is moment tensor which constitute seismic moment tensor inversion (SMTI) technique. Seismic moment tensors contain valuable information about source mechanisms, however, without certainty about the fracture plane orientation and the slip direction as SMTI solution provides two equally possible failure planes.

Stress inversion is a methodology that recovers additional information about stress state of the failure mechanisms and was researched by many authors (e.g., Gerhart & Forsyth 1984; Michael 1984; Vavryčuk 2014). In this paper we used stress inversion approach of Vavryčuk (2014) to determine principal stresses direction and resolve failures plane orientation.

5 Dataset

As mentioned earlier, the underground block caving mine discussed in this study locates in tectonically active area and induced seismicity level from the other hand is relatively high as well. So, three months of microseismic monitoring data was used in this study and the number and spatial location of microseismic events ensured good resolution and applicability of advanced microseismic analysis methods. These three months of monitoring include peak mine production activity and a short period of relative inactivity.

The data was divided into six temporal groups, where each group represents microseismic activity before a relatively large microseismic event occurrence with moment magnitude above 0.5. Thus, the microseismic data in each group relates to stress redistribution in the cave abutments contributing to the large microseismic event occurrence and stress release. The first two time groups relate to constant high mining production rate and the microseismic events within last four temporal groups correspond to relative production inactivity period.

Based on the approach, the total number of microseismic events used for advanced analysis reflected the input data quality requirements. So, approximately 20,000 accurately located, good quality microseismic events were used in seismic tomography analysis to maximize image resolution. Only low magnitude cut off M_w = -1.8 was applied to the data set. For DPA, the events with moment magnitudes M_w

between -1.6 and 0.5 were used. The restriction on high moment magnitudes is due to seismic network geophone's specifications – the minimum recorded frequency for the majority of microseismic events is 15 Hz that doesn't allow accurate estimation of the source parameters for the events with Mw > 0.5. For microseismic events with moment magnitudes M_w below -1.6, waveform background noise level affects spectral analysis and therefore accurate source parameters assessment. After magnitude filter application, there were about 2,000 events per temporal group available for DPA analysis. For stress inversion, only high quality microseismic events with well resolved seismic moment tensor mechanisms were used. SMTI requirements applied to the whole data set, left about 300 events per temporal group for stress inversion.

6 Rock characterization using advanced microseismic analysis

The first method applied to the dataset was DPA. All three indices were computed for each time group, normalized and presented on ternary plots (Figure 1), where each corner of the triangle represents the maximum value of the specific dynamic parameter.

DPA shows that during the selected 3-month time period the rock mass surrounding the cave went through a cycle of loading and relaxation returning to approximately the same state of stress and co-seismic deformation as the SI and PI of groups 1 and 6 are similar.

During time group 2, a number of microseismic events occurred, including some of the relatively high magnitude events, which caused noticeable stress release with a relatively constant level of plastic deformation. The stress field gradually recovered through time groups 3, 4 and 5, returning to the original level related to peak production (time group 1).

During time group 6 the rock mass went through a stress loading and relaxation cycle, with SI variations comparable to those happened during the previous five time groups, which indicates relative stability of the steady state intensity of the rock stress field around the cave.

Calculated 3D fields of PI, DI and SI distribution in the rock around the cave were later analyzed together with travel time tomography velocity variation models and stress inversion results.

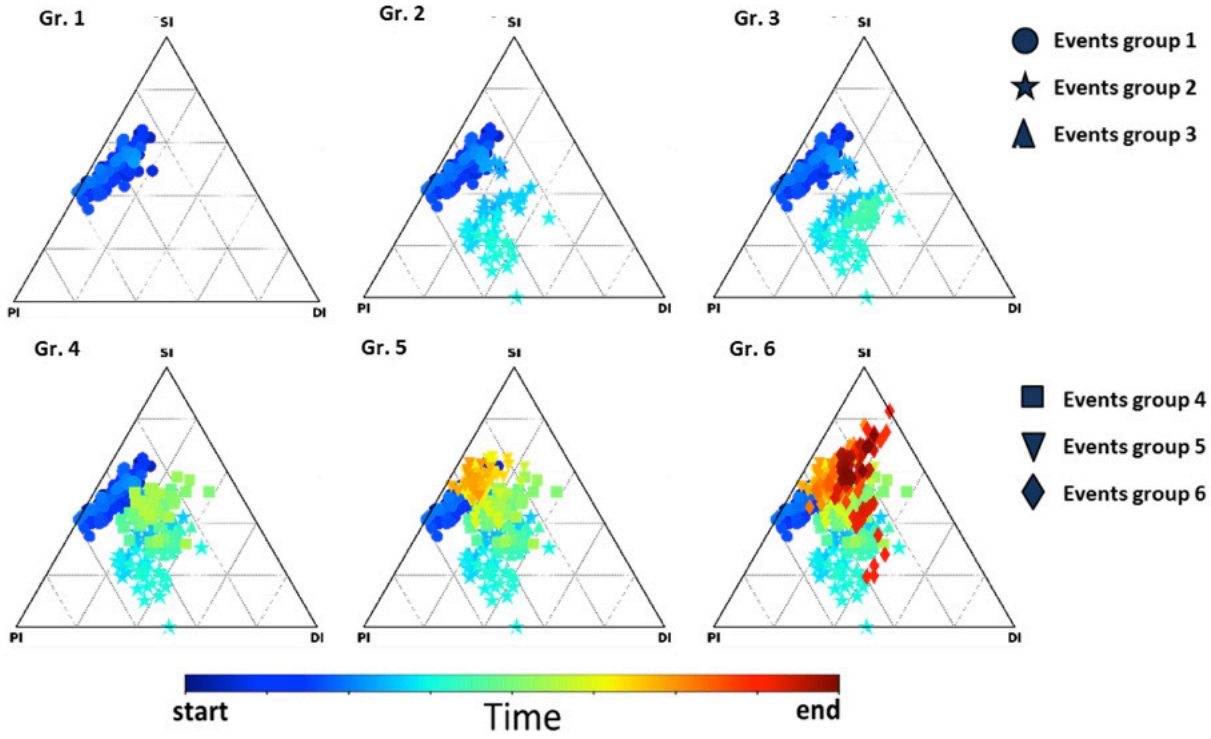

Figure 1 Stress loading and relaxation cycle of the rock mass surrounding the cave presented on the ternary plots for each time group

The second methodology we applied in this study was passive seismic tomography. We used two starting velocity models for travel time tomography: a homogeneous velocity model and a 3D velocity model. The results can be used to assess the structural imprint versus stress variation with time. Figures 2 and 3 show the results of the P-wave tomography. Figure 2 shows plan view of the velocity cube at the cave base depth using the homogeneous initial velocity model and Figure 3 shows plan view at the cave base depth of the velocity cube using the 3D initial velocity model.

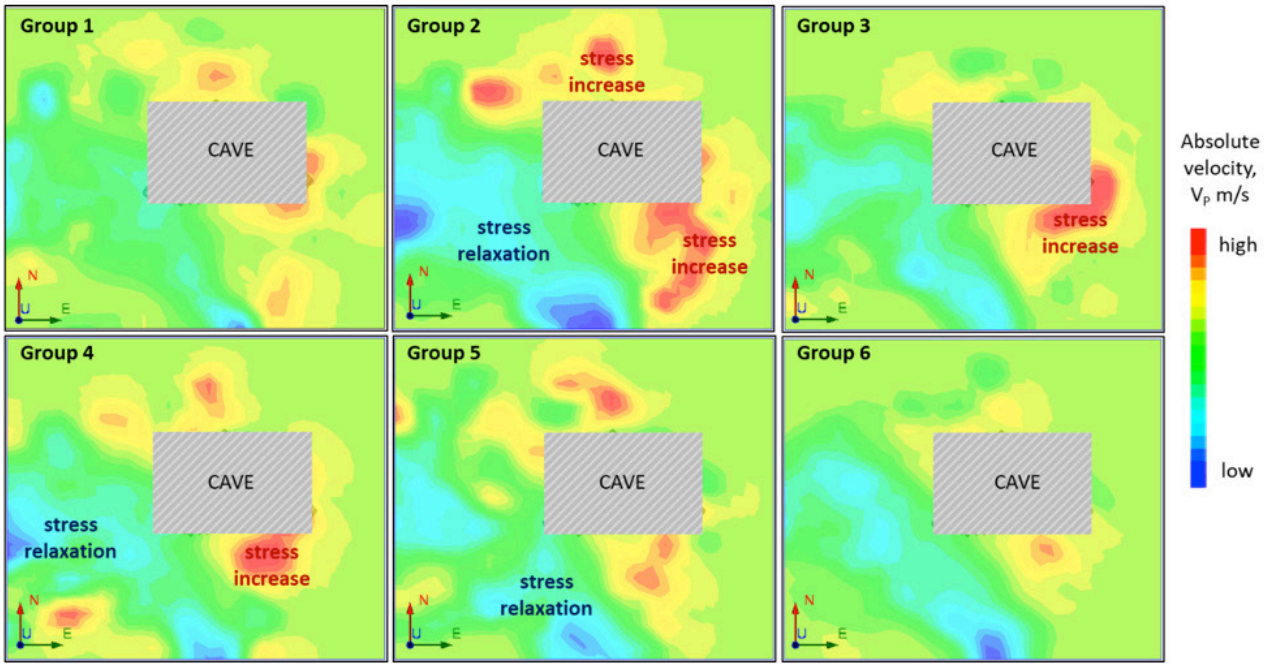

Figure 2 **Tomography results using an initial homogeneous velocity model. Each image presents horizontal cross section through the inverted velocity cube for every time group**

Both initial models resolve identical patterns of velocity change with time. However, in case of homogeneous initial velocity model, the velocity variation range of the final model appears larger than in case of 3D initial velocity model tomography. The difference is partially caused by a structural imprint of a high velocity zone of an intrusion that crosses the mine area.

In the mining environment, an increase in compressional velocity usually indicates an increase in stress (de Beer et al. 2018; Verdon et al. 2008; Price et al. 2017). Both initial models result in tomographic images showing local stress increase for time groups 3, 4 and 5 on the south-eastern abutment of the cave. This result correlates with the DPA indicating stress loading processes during this time period. DPA and seismic tomography are independent methods, that confirm each other's results and bring additional evidence, for example, DPA includes data about deformability and rock failure complexity while tomography offers information about stress evolution in the areas of rock mass devoid of seismicity or recording sensors.

The third part of this study is the determination of the principal stress directions from seismic moment tensor mechanisms of the microseismic events. The moment tensor mechanisms themselves were evaluated allowing for a general seismic moment tensor solution and not constraining the solution to be solely from a double-couple source. The Hudson's source plot (Hudson et al. 1989) is used for visualization of rock failure mechanisms decompositions. Figure 4 shows source mechanism plots for microseismic events from time group 1. The tomography velocity distribution is mapped in the background to enable visualizing the position of high velocities within the rock mass.

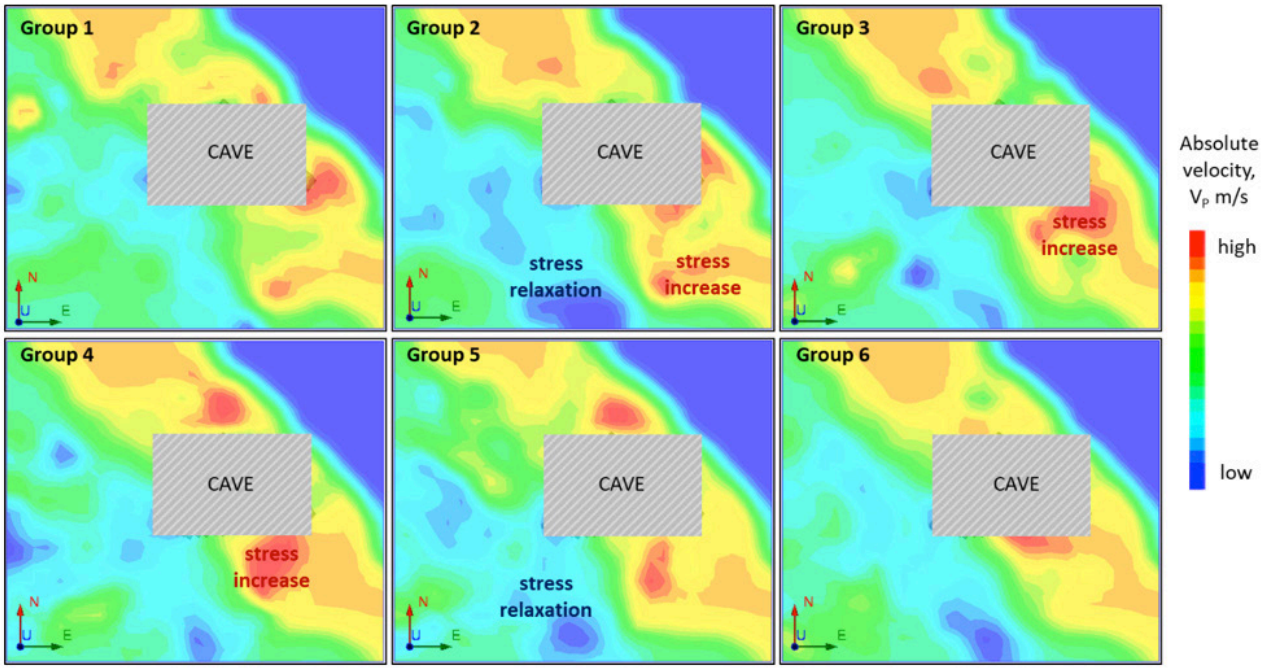

Figure 3 Tomography results using an initial 3D velocity model. Each image presents horizontal cross section through the inverted velocity cube for every time group

The dominant failure mechanisms on the south and the east sides of the mine are shear-tensile crack closing, which is consistent along the whole south and east walls of the cave. In the north and northwest abutments of the cave, events have tensile crack closing failure mechanisms with volume collapsing components (sliding). Tensile crack opening mechanisms are not as common and appear to be present only in events from the south-west abutment of the cave.

Figure 5 displays the results of the stress inversion for the microseismic events in time group 1. The main stresses σ1, σ2 and σ3 are presented as stars on the stereonet plots and correspond to the source type plots on Figure 4.

The main stress directions change around the cave, confirming complexity of the caving-induced stress distribution. Only the σ1 stress direction along the south abutment of the cave does not change much with time and maintains vertical and semi-vertical orientation through all three months monitoring period. The σ1 stress orientation rotates semi-horizontally and towards the north and northwest along the west and north abutments of the cave where several different geotechnical domains are present. Such behaviour observed in time group 1 events is similar to the other time groups. Most of the variation of the σ1 stress direction with time is observed along the east abutment of the cave.

As for the rock failure planes orientation, most of the planes are vertical and sub-vertical (see Figure 6) with strike direction from E-W to N-S. All fault planes for all the microseismic events in the group represented by their poles and plotted on the stereonets as variable density areas with hot colours representing high concentration of poles. One dominant fault plane is selected by the highest poles concentration and is presented by white great circle on the stereonet.

Fault planes of the south and west abutments of the cave are vertical and sub-vertical and have alike NE-SW strike. Dominant rock failure planes in the south-east abutment of the cave have N-S and E-W strike in the north-west and north-east abutments of the cave.

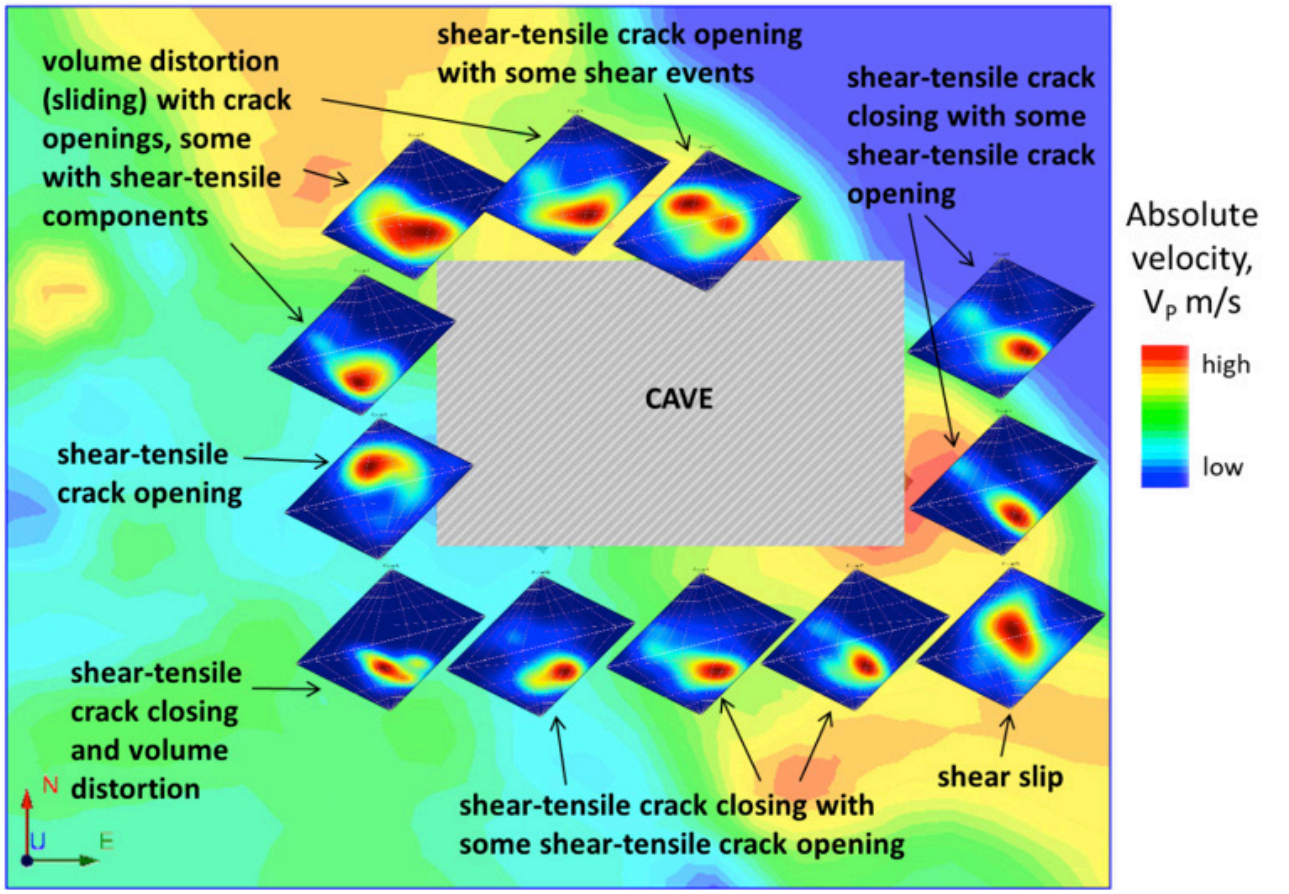

Figure 4 Hudson source plots of seismic moment tensor mechanisms of microseismic events from time group 1 around the cave superimposed on the compressional velocity map from the 3D seismic tomography

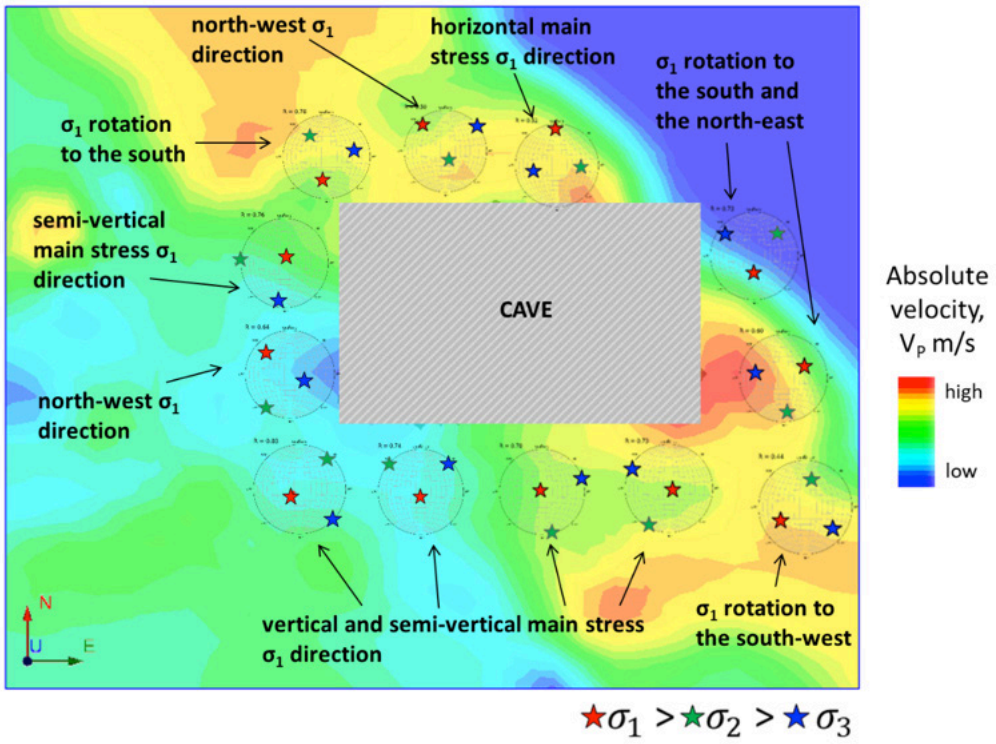

Figure 5 Stress inversion results (main stress directions) for time group 1 microseismic events superimposed on top of the compressional velocity map from the 3D seismic tomography

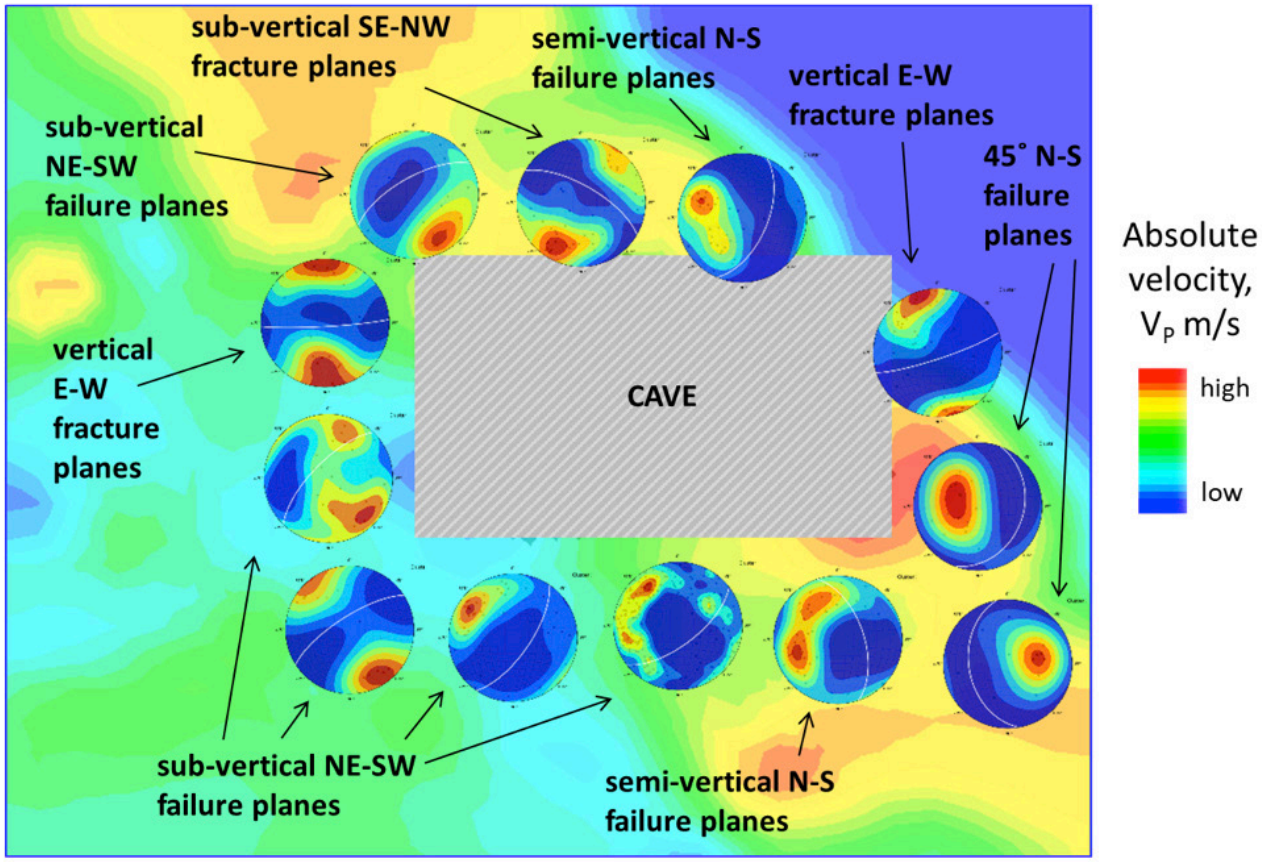

Figure 6 **Rock failure planes orientation for time group 1 microseismic events superimposed on top of the compressional velocity map from the 3D seismic tomography**

7 Conclusions

In this study we used three independent advanced microseismic analysis approaches to characterize cave mining related stress field and its evolution during and after the peak production activity.

These approaches – DPA, passive seismic tomography and stress inversion – provide complementary information for interpretation of the complex spatial and temporal stress field evolution. DPA showed a cyclical process of loading and stress relaxation in the abutments of the cave during the period of study. Seismic tomography recovered compressional velocity variations correlating with the stress field behaviour observed in DPA. The region of high velocity within the rock mass seems to undergo a loading process with local stress increase, while the region of low velocity rock mass on the south-west side of the mine undergoes stress relaxation with high intensity plastic deformation.

Seismic moment tensor mechanisms show uniformity in the south abutment of the cave - tensile crack closure – and coincide with the region of low velocity. The high velocity region exhibits some tensile fracture opening with consistent tensile fracture closure failure type along the south and east abutments of the cave.

The main stress directions vary around the mine and seem to have additional level of complexity related to vertical distribution of the events. The maximum principal stress $\sigma 1$ in the south abutment of the cave appears to be consistently vertical.

As for the rock failure planes – their dominant dip orientation is vertical, and strike is varying from E-W to N-S. South abutment of the cave has relatively consistent sub-vertical EN-SW main fracture planes.

References

Baig, AM, Bosman, K & Urbancic, TI 2017, 'Temporal changes in stress state imaged through seismic tomography', in J Wesseloo (ed.), Proceedings of the Eighth International Conference on Deep and High Stress Mining, Australian Centre for Geomechanics, Perth, vol. 1, pp. 269–273.

Ben-Zion, Y 2008, 'Collective behaviour of earthquakes and faults: Continuum-discrete transitions, progressive evolutionary changes, and different dynamic regimes', Reviews of Geophysics, vol. 46, no. 4, RG4006, https://dx.doi.org/10.1029/2008RG000260

Crowley, JW, Baig, A & Urbancic, T 2015, '4D tomography and deformation from microseismic data', Proceedings of the 85th Annual Meeting of the Society of Exploration Geophysics, Society of Exploration Geophysicists, Tulsa.

de Beer, W, Smith-Boughner, L, Viegas, G, Bosman, K & Angus, D 2018, 'Towards physics-based hazard assessment tools for developing blanket re-entry rules', in Y Potvin & J Jakubec (eds), Proceedings of the Fourth International Symposium on Block and Sublevel Caving, Australian Centre for Geomechanics, Perth, pp. 545-552.

Gephart, JW & Forsyth, DW 1984, 'An improved method for determining the regional stress tensor using earthquake focal mechanism data: application to the San Fernando earthquake sequence', Journal of Geophysical Research, vol. 89, no. B11, pp. 9305–9320. http://dx.doi.org/10.1029/JB089iB11p09305.

Hudson, JA, Pearce, RG & Rogers, RM 1989, 'Source type plot for inversion of the moment tensor', Journal of Geophysical Research: Solid Earth, vol. 94, no. B1, pp. 765–774.

Kostrov, BV & Das, S 1988 'Principles of Earthquake Source Mechanics', Cambridge University Press, Cambridge.

Ma, X, Westman, EC, Fahrman, BP & Thibodeau, D 2016, 'Imaging of temporal stress redistribution due to triggered seismicity at a deep nickel mine', Geomechanics for Energy and the Environment, vol. 5, pp. 55–64.

Mercier, J-P, de Beer, W, Mercier, J-P & Morris, S 2015, 'Evolution of a block cave from time-lapse passive source body-wave travel time tomography', Geophysics, vol. 80, no. 2, pp. WA85–WA97, https://dx.doi.org/10.1190/geo2014-0155.1

Michael, AJ 1984, 'Determination of stress from slip data: faults and folds: Journal of Geophysical Research, vol. 89, no. B13, pp. 11517–11526. http://dx.doi.org/10.1029/JB089iB13p11517.

Price, D, Angus, DA, Garcia, A. & Fisher, QJ 2017, 'Probabilistic analysis and comparison of stress-dependent rock physics models', Geophysical Journal International, vol. 210, no. 1, pp. 196-209.

Smith-Boughner, L, Urbancic, T & Baig, A 2017, 'Resolving sill pillar stress behaviour associated with blasts and rockbursts', in J Wesseloo (ed.), Proceedings of the Eighth International Conference on Deep and High Stress Mining, Australian Centre for Geomechanics, Perth, pp. 257–267.

Urbancic, T, Smith-Boughner, L, Crowley, JW, Viegas, G, Baig, A & von Lunen, E 2015, 'Characterizing the dynamic growth of a fracture network', Proceedings of the Unconventional Resources Technology Conference, Society of Petroleum Engineers, Richardson, http://dx.doi.org/10.15530/URTEC-2015-2154641

Vavryčuk, V 2014, 'Iterative joint inversion for stress and fault orientations from focal mechanisms', Geophysical Journal International, vol. 199, pp. 69-77.

Veigas, G, Bosman, K, Angus, D, de Beer, W, & Urbancic, T 2018, 'Mapping cave front growth utilising the collective behaviour of seismicity and velocity fields', in Y Potvin & J Jakubec (eds), Proceedings of the Fourth International Symposium on Block and Sublevel Caving, Australian Centre for Geomechanics, Perth, pp. 577-588.

Verdon, JP, Angus, DA, Kendall, J-M & Hall, SA 2008 The effect of microstructure and nonlinear stress on anisotropic seismic velocities, Geophysics, vol. 73, no. 4, pp. D41- D51.

Westman, E, Luxbacher, K & Schafrik, S 2012, 'Passive seismic tomography for three-dimensional time-lapse imaging of mining-induced rock mass changes', The Leading Edge, vol. 31, pp. 338–345.

Young, R, & Maxwell, S 1992, 'Seismic characterization of a highly stressed rock mass using tomographic imaging and induced seismicity', Journal of Geophysical Research, vol. 97, pp. 12361–12373.